3B2v7.51c GML4.3.1 | Emas : 01064 | Prod.Type: pp.1–14(col.fig.:NIL) | ED: PAGN: thara SCAN:

Collisional Activation and Dissociation: Via Ion-neutral Complexes

1. Theory

1.1 Planetary Motion

Ion–neutral complexes intervene in a wide variety of unimolecular and bimolecular ionic reactions in the gas phase. This article deals with unimolecular decompositions that occur in ionized organic molecules. Most compounds exhibit a large number of peaks in their fragmentation patterns, both in the ion source and under conditions of collisionally activated decomposition. Dissociations via transient, noncovalent intermediates (i.e., ion–neutral complexes) contribute minor peaks in many systems and the dominant peaks in a few. The scope of ion–neutral complex-mediated pathways has yet to be fully explored. The discussion below focuses on a handful of examples that have been closely studied.

In the gas phase, chemical species can move like heavenly bodies. Because an ion and a neutral attract one another, they may enter orbit around their center of mass. If, however, they behave like the Earth–Sun system, the rotation of each body should be independent of their revolution about one another (e.g., the difference between a day and a year). A neutral with a large permanent dipole moment might exhibit locked rotation (like the Moon, which keeps one face pointed towards the earth, so that a day on the moon lasts a month). In any event, the rotation and revolution of the ion should be virtually independent of one another. "Planetary motion" of an ion and a molecule has been proposed on the basis of theoretical models, and transient intermediates that obey this description have been characterized experimentally. Such intermediates are called ion–neutral (or ion–molecule) complexes. There is evidence to implicate ion–neutral complexes in decompositions of singly charged parent ions produced by all types of ionization under all sorts of dissociation conditions.

A simple example of planetary motion for a stable molecular species has been described for the cluster of Li^+ with a molecule of tetrahedral elemental phosphorus (<Bib1>*1*), which can be represented as [P_4 Li^+]. The molecular fragment has no permanent dipole, so its rotation does not exert a large effect on the attractive potential between it and the ion. At room temperature, the average internal energy of [P_4 Li^+] is calculated to be greater than the barrier height for turning the P_4 in any direction. In other words, there is little directed valence between P_4 and Li^+. Whatever attraction exists between them does not have much covalent character. The term "electrostatic bonding" is sometimes used in order to signify that changes of orientation of one partner relative to the other have little effect beyond what would be predicted by classical ion–dipole and ion–induced dipole forces.

The cluster of ammonium ion with hydrogen fluoride, $NH_4^+ \cdots FH$, displays a higher degree of complexity (<Bib2>*2*), because the ion and the neutral can both rotate. At low internal energies, the fluorine is hydrogen bonded to one of the ammonium hydrogens and the attraction between them exhibits directionality. With only a small amount of internal excitation, the ammonium ion starts to rotate independently of the HF molecule, even though the latter remains with its dipole pointed towards the electric charge. In this "planetary" system, the ion plays the role of the Earth and HF the role of the Moon.

1.2 Constraints Imposed by Conservation of Angular Momentum

Although the $NH_4^+ \cdots FH$ cluster ion has yet to be observed experimentally, the proton-bound dimer of ammonia with fluoromethane, $NH_4^+ \cdots FCH_3$, has been seen in the mass spectrometer (<Bib3>*3*). Here, planetary motion should have an energy barrier comparable to the barrier to internal rotation about single bonds. Unlike the more familiar case of internal rotation (which is a one-dimensional motion about an interatomic axis), planetary motion includes free movement about axes perpendicular to the interfragment axis.

Planetary motion can be considered as the large-amplitude limit of a bending vibration. Consider $NH_4^+ \cdots FCH_3$ with zero net angular momentum. Figure 1 portrays classical descriptions of symmetric (a) and antisymmetric (b) bends of hydrogen-bonded $NH_4^+ \cdots FCH_3$ in the plane of the page, where each set of arrows stands for a phase of the relative classical motions. A linear combination of these two vibrations, (a) + (b), gives libration of the ammonium ion by itself about an axis perpendicular to the H···F hydrogen bond, (c). In (c) the double-headed arrow symbolizes the rocking back and forth of the ion at the same time as the F—C dipole remains pointed towards the positive charge. The representations in Fig. 1 do not include small displacements of the centers of mass of NH_4^+ and of FCH_3 away from their equilibrium positions, which are necessary if there is to be no torque associated with these bending vibrations. In the large amplitude limit of Fig. 1(c) the ammonium ion turns 360°, and the compensatory displacements of the individual centers of mass also execute 360° turns, as illustrated by Fig. 1(d). The net result is free rotation of the ammonium ion accompanied by revolutions of the individual centers of mass so as to keep the total angular momentum constant in exciting from (c) to (d). These compensatory motions of the centers of

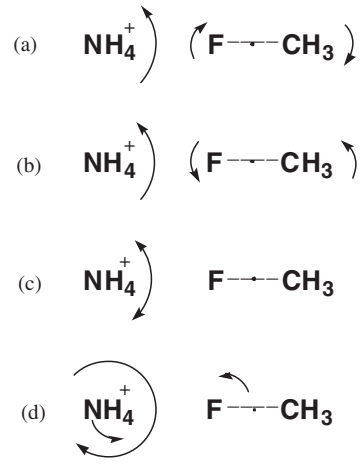

Figure 1
Two normal modes of the ammonium–fluoromethane system with zero angular momentum: a symmetric bend (a) and an asymmetric bend (b), along with their superposition (c), corresponding to (a) minus (b). The center of mass of fluoromethane is represented by a heavy dot, and (d) represents the large amplitude limit of (c), where conrevolution of the individual centers of mass of the ammonium ion and the fluoromethane (symbolized by small arrows) compensates for the angular momentum of rotation of the ammonium ion about an axis perpendicular to the plane of the page.

mass, which have the same helical sense as each other but run opposite to the rotation of the ammonium ion, have been termed "conrevolution."

SX040 The same sort of motions can take place in the plane perpendicular to the page (and the interfragment axis). The net extent to which conrevolution operates is dictated by conservation of angular momentum. It depends on the overall angular momentum J of the system and the degree of coupling between J and the angular momentum of NH_4^+ by itself. In any event, excitation from (c) to (d) corresponds to a transition from directed valence to planetary motion.

SX045 Equilibrium measurements on the gas-phase association reactions $AH^+ + B \lambda B—AH^+$ give evidence for the increase in entropy that accompanies conversion of covalent to electrostatic bonding. In cases where experiment implies the existence of two different $B—AH^+$ isomers, the values of ΔH and ΔS give only a hint as to their structures. For either isomer, the enthalpy and entropy of association are both negative. Nonlinear van't Hoff plots of log K_{eq} versus $1/T$ have been analyzed in terms of a pair of intersecting lines. At lower temperatures the linear relationship has greater slope (corresponding to a more exothermic association of the ion AH^+ with the neutral base B), which is inferred to correspond to covalent association. At higher temperatures, the slope is not as steep, which means that the bonding is weaker energetically, but the intercept corresponds to an entropy of association that is less negative (<Bib4>*4*), consistent with freely rotating fragments.

In order to get a better idea of the nature of SX050 noncovalent bonding, one must look to the products of dissociation reactions. The data suggest that, in many cases, singly charged ions pass through transient ion–neutral complexes en route to the observed fragments. Cleavage of a covalent bond to form an ion–neutral complex transforms five vibrations into five looser degrees of freedom: two librations of the neutral partner in planes perpendicular to the interfragment axis (e.g., the motion of the FCH_3 in Figs. 1(a) and (b), which may have sufficient amplitude also to be 360° rotations), planetary motion of the ion (as typified by Fig. 1(d) combined with the orthogonal rotation perpendicular to the page, which accounts for two more degrees of freedom), and radial motion of one partner relative to the other. Quantum mechanically, no closed-form solution has been found to describe these last degrees of freedom, even in the simplest central force approximation (a point charge–point induced dipole), but the density of states can be estimated for a given domain of ion–neutral distances. The increase in entropy associated with creating an ion–neutral complex compensates for the energetic cost, "the stabilization–rotation compromise" (<Bib5>*5*). More importantly, once an ion–neutral complex forms, reforming the covalent bond encounters an entropic bottleneck, which slows the rate of reversion, even if no energy barrier exists to prevent this collapse.

1.3 Unimolecular Versus Bimolecular Regimes SX055

Consider a hydrogen atom abstraction reaction between a methyl radical ($CH_3\cdot$) and an even-electron ion (AH^+). Let us suppose that the approach of $CH_3\cdot$ and AH^+ is barrier free when the system has no net angular momentum ($J=0$), as represented by the lower dashed curve in Fig. 2. The minimum of this incoming curve will be assumed to have the covalent structure $CH_3AH^{\bullet +}$. Let us further suppose that there is just one local maximum for the outgoing potential when $J=0$ (as depicted by the solid curve in Fig. 2), corresponding to the activation energy for atom abstraction. The outgoing potential corresponds to the reaction coordinate for making the products, CH_4 and $A^{\bullet +}$.

If the two reactants encounter one another in a SX060 bimolecular collision, the system usually has a substantial angular momentum (large J), and there will be additional energy barriers resulting from the repulsive centrifugal potential (<Bib6>*6*). The upper dashed curve in Fig. 2 represents the effective

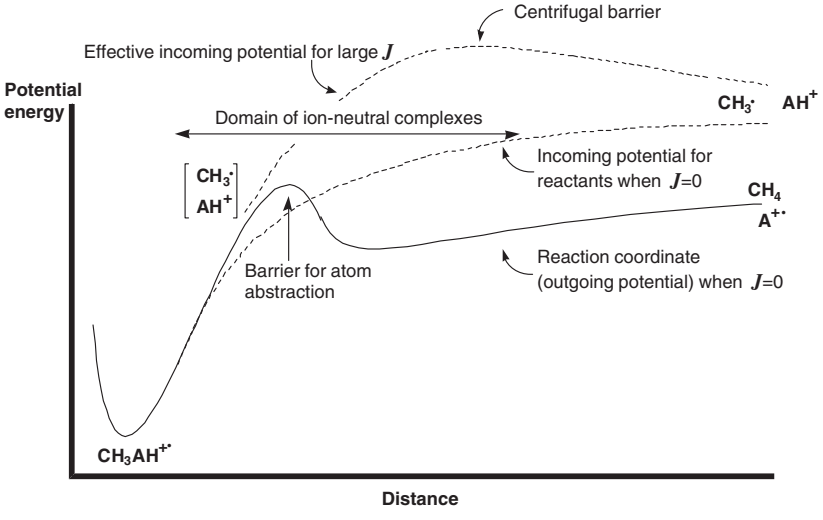

Figure 2
Potential energy curves for hydrogen atom abstraction from $AH+$ by a methyl radical. The lower dashed curve represents the attractive incoming potential between $CH_3\cdot$ and AH^+, the solid curve depicts the reaction coordinate for atom abstraction when the angular momentum equals zero, and the upper dashed curve represents the effective incoming potential when the angular momentum is large.

incoming potential for the bimolecular encounter for nonzero J (cf. Chapter 1 of this volume). The height of the centrifugal barrier depends on rotational state, although the $J=0$ curve and the large J curve merge at long distances.

SX065 For unimolecular decomposition of a thermally equilibrated precursor ($CH_3AH^{\bullet+}$), the average rotational level at 300 K is so low that the centrifugal barrier height will be of the order of $1\,cm^{-1}$. Thus the effective potentials are virtually the same as the $J=0$ curves. For bimolecular reactions (large J), an ion–neutral complex can be imagined as an intermediate somehow trapped to the right of the centrifugal barrier. In other words, when an ion and a molecule attract one another from afar, a potential energy maximum stands between them and their covalently bound aggregate. In this regime, the reactants may spend time in one another's vicinity even if they cannot surmount the potential energy barrier. By contrast, for a unimolecular reaction, the domain of ion–neutral complexes does not require that a potential energy barrier separate the complex from its covalent precursor $CH_3AH^{\bullet+}$. If two reactants, $CH_3\cdot$ and AH^+, were coming together on the lower dashed curve, they would need to stop rotating in order to form a covalent bond. A locked-rotor critical configuration would have to intervene, even in the absence of a potential energy barrier. For a unimolecular decomposition, two separating polyatomic cleavage fragments go out on the same curve as for their association and pass through the same type of bottleneck.

Ion–neutral complexes represent transient intermediates that have separated past that locked-rotor critical configuration, but which do not have enough translational kinetic energy to continue out to very large separation. The complex may have a total kinetic energy content well in excess of what is needed to separate the fragments, but if sufficient energy is not deposited into the translation of one fragment relative to the other, they are stuck for a brief interval in the domain represented by the double-headed arrow in Fig. 2. In many cases, this sojourn may last long enough for the fragments to find a competing exit pathway (such as represented by the solid curve in Fig. 2). SX070

Scheme 1 compares simple cleavage of $CH_3AH^{\bullet+}$ with formation of an ion–neutral complex. Simple dissociation of $CH_3AH^{\bullet+}$ to $CH_3\cdot$ and AH^+ has a positive translational kinetic energy release T, whereas formation of an ion–neutral complex can be viewed as corresponding to a negative translational kinetic energy release, $T<0$. In other words, SX075

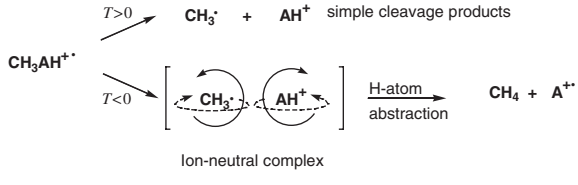

Scheme 1

the kinetic energy imparted to the fragments is not sufficient to overcome their mutual attraction. If the kinetic energy release $T>0$ has a sufficiently small absolute value, then the fragments start to rotate relative to one another (as the dashed and curved arrows in Scheme 1 represent). Methyl radical has no dipole moment and a nearly isotropic polarizability, so both it and the ion can rotate independently of one another (subject, of course, to conservation of total angular momentum).

SX080 Rotations around axes perpendicular to the inter-fragment direction reduce the probability for reforming the covalent bond. In an $[CH_3\cdot\ AH^+]$ ion–neutral complex, the *p* orbital containing the unpaired electron of the methyl radical would have to point towards a vacant orbital of AH^+ in order to return to $CH_3AH^{\bullet+}$. Likewise, a vacant orbital of AH^+ would have to point towards the methyl radical. The dashed and solid curved arrows in Scheme 1 represent four degrees of freedom that are essentially free rotations, and freezing them in order to reform $CH_3AH^{\bullet+}$ diminishes the density of states substantially, thereby reducing the entropy. This entropic barrier to such a collapse gives the complex a lifetime long enough for the atom abstraction to take place.

SX085 The question arises whether ion–neutral complexes operate primarily when there is not enough energy for bond cleavage. This issue has been addressed in the case of ionized acetamide. A density-of-states model has been marshaled for the keto form of the ion, $CH_3CONH_2^{\bullet+}$, to predict the probability of forming a $[CH_3\cdot\ AH^+]$ ion–neutral complex relative to the probability of simple bond fission (<Bib7>*7*), where AH^+ stands for N-protonated isocyanic acid, $H_2N=C=O^+$. This model argues that ion–neutral complexes need not be restricted to an energy range where the precursor ion has less energy than the dissociation threshold. In other words, ion–neutral complexes form even when $CH_3AH^{\bullet+}$ has an internal energy content considerably in excess of any centrifugal barrier to its dissociation. The anticipated experimental outcome from $[CH_3\cdot\ AH^+]$ is atom abstraction, leading to $HN=C=O^{\bullet+}$ as the ion $A^{\bullet+}$ observed in the mass spectrometer as a consequence of CH_4 elimination.

SX090 At the time the density-of-states model was first proposed (<Bib8>*8*), methane expulsion from ionized acetamide had never been reported (largely because the fragment ion is isobaric with $CH_3C\equiv O^+$, a very prominent peak in the mass spectrum of acetamide). High-resolution mass spectrometry using 70 eV electron ionization gives an observed abundance of $HN=C=O^{\bullet+}$ about 0.04 the intensity of $H_2N=C=O^+$ (the base peak, which comes from $CH_3\cdot$ loss), as compared to a predicted abundance of 0.1 from the density-of-states model for $J=0$. The comparison of theory with experiment is complicated by the fact that electron ionization of acetamide yields a mixture of two isomeric molecular ions (the enol tautomer $CH_3C(OH)=NH^{\bullet+}$ is about twice as abundant as the keto form) (<Bib9>*9*). The extent to which the density-of-states model agrees with measured peak intensities suggests that ion–neutral complexes form even when the precursor ions have high vibrational energy contents.

The metastable ion decomposition of ionized ^{15}N-labeled acetamide (where the ion from methane loss no longer has the same nominal mass as $CH_3C\equiv O^+$) exhibits the same abundance of $[M—CH_4]^{\bullet+}$ relative to $[M—CH_3]^+$ as is seen in the 70 eV source mass spectrum. The timescales of these two types of mass spectrometric measurement differ greatly (as, one presumes, do the internal energy distributions of the decomposing ions). The apparent insensitivity of the $[M–CH_4]^{\bullet+}/[M—CH_3]^+$ intensity ratio to internal energy confirms the conclusion that ion–neutral complexes can intervene over a wide domain of internal energies. SX095

2. *Experiment* SX100

2.1 Alkane Elimination: Homolytic and Heterolytic Mechanisms

Alkane eliminations, which occur from both even- and odd-electron organic ions, represent a class of unimolecular ion decompositions where ion–neutral complexes operate (<Bib10>*10*). Scheme 1 depicts a case that has been generalized for a variety of odd-electron ions, when an alkyl radical $R\cdot$ is put in place of methyl. Photoionization studies of alkane eliminations show that they can compete effectively with production of $R\cdot$ from a number of gaseous radical cations, even at energies considerably above the thermodynamic threshold for simple cleavage (<Bib11>*11*).

Scheme 1 exemplifies a homolytic mechanism. That is to say, the charge localized on the AH^+ part of the reactant remains on that fragment when the bond breaks. Alkane eliminations from even-electron reactants tend to operate via heterolytic mechanisms, i.e., where charge localized in one region of the reactant shifts to the other fragment after cleavage. Scheme 2 portrays such a pathway, as has been demonstrated for decompositions of gaseous alkoxide ions (<Bib12>*12*). Although it is likely that electric charge delocalizes to some extent between the partners in an ion–neutral complex, the rearrangement chemistry outlined later in this section makes it clear that the distinction between homolysis and SX105

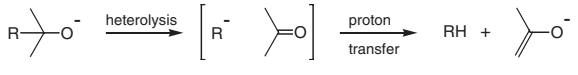

Scheme 2

heterolysis has meaning in the context of ion–neutral complexes.

SX110 Another instance of heterolysis of an even-electron ion leading to alkane expulsion occurs in chemically ionized aromatic hydrocarbons. Extensive studies of systems in which two benzene rings are separated by an alkyl chain (as Scheme 3 exemplifies) demonstrate that ion–neutral complexes intervene. Hydrogens scramble very rapidly among the sp^2 centers in protonated aromatic systems (both within rings and between rings) (<Bib13>*13*), so it does not matter where H^+ is initially deposited. Protonation *ipso* to a *t*-butyl group leads to heterolysis, forming an ion–neutral complex containing a *t*-butyl cation. When the two rings of the neutral partner are identical within the complex (e.g., R = methyl, R′ = H), subsequent hydride abstraction occurs to equal extents from the α- and γ-positions. When the two rings are different, hydride abstraction to expel isobutane favors the position that gives the more stable benzylic cation (as when R = H and R′ = methyl, where deuterium labeling shows a 16:84 ratio of α- to γ-abstraction) (<Bib14>*14*).

SX115 Alkane elimination may occur in competition with alkene elimination. This is seen in the chemical ionization of ketones with CF_4 reagent gas. Electron ionization of CF_4 produces CF_3^+ ions, which attach to the carbonyl oxygen with an exothermicity of the order of $\Delta H = -3$ eV. For acyclic ketones with more than three carbons, the resulting vibrationally excited adduct ions decompose principally via expulsion of neutral hydrocarbon molecules. In the case of isobutyl ethyl ketone, $(CH_3)_2CHCH_2COCH_2CH_3$, about one-fourth of the adduct ions heterolyze to form ion–neutral complexes, as Scheme 4 depicts. These complexes expel propane to yield the allylic *m*/*z* 139 ion shown in Scheme 4 (whose structure has, in turn, been characterized by its collisionally activated decomposition pattern) (<Bib15>*15*) about twice as often as they expel propene to give *m*/*z* 141 ions.

Ion–neutral complexes intervene as transient intermediates in many other unimolecular and bimolecular (ion–molecule) reactions. For historical reasons, the best-studied examples have been unimolecular decompositions of positive ions produced by electron, photo-, or chemical ionization of gaseous molecules. There is evidence for ion–neutral complexes (of both charges) in collisionally activated dissociation of ions electrosprayed from solution. SX120

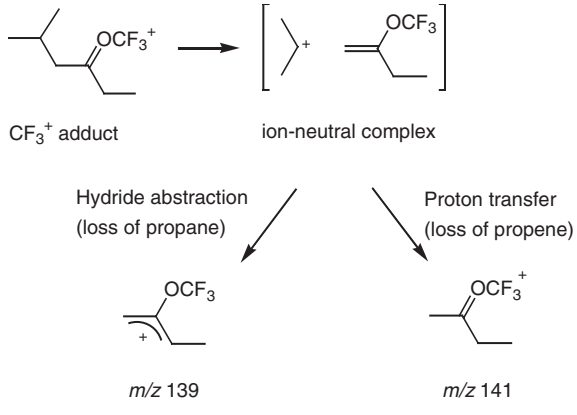

Scheme 4

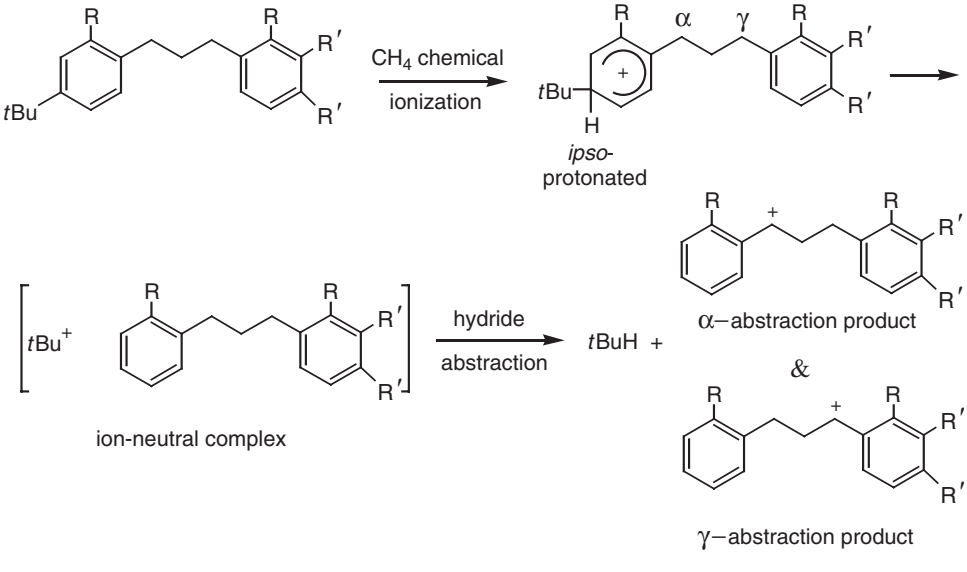

Scheme 3

Complex-mediated reactions have been observed on timescales as brief as 10^{-11} s.

SX125 *2.2 The Reorientation Criterion*

When a neutral reactant cleaves, very weak forces hold the uncharged fragments together. These forces fall off rapidly with distance. At separations of a few angstroms the residual binding energy is typically $<kT$ at room temperature. In condensed phases, solvent or matrix molecules can hem in cleavage fragments and impede their escape from one another. This is called a cage effect. In the gas phase no such restraint prevents neutrals from rapidly separating from one another once covalent bonds have broken.

SX130 If one of the cleavage fragments carries net electric charge, ion–dipole and ion–induced dipole attraction falls off more slowly (cf. Chapter 1 of this volume), providing an electrostatic leash that often prevents their rapid separation, even in the absence of any solvent. This "leash effect" represents a gas-phase equivalent of the cage effect in condensed phases (<Bib16>*16*). Not all gas-phase ion dissociations pass through ion–neutral complexes. One sort of experimental evidence for a "leash effect" comes from dissociations that require a fragment within the complex to turn about an axis perpendicular to the broken bond, analogous to the large radius rotation shown in Fig. 1(d). Reactions that display this behavior are said to fulfill the reorientation criterion for inferring intermediacy of ion–neutral complexes (<Bib17>*17*).

The four examples below illustrate unimolecular ion dissociations of radical cations that meet the reorientation criterion (where the dashed arrows represent the reorientations). Scheme 5 portrays the decomposition of an ionized steroidal diamine, which demonstrates the reorientation of a neutral fragment that is much heavier than the ion (analogous to the planetary motion within $[P_4\ Li^+]$). Cleavage of a carbon–carbon bond of the molecular ion gives a neutral radical and an even-electron iminium ion. Reorientation of the radical brings the other nitrogen close enough to the iminium ion that proton transfer takes place, leading to expulsion of neutral $CH_3CH=NH$ and formation of a distonic ion (<Bib5>*5*) (see *Organic Ion Chemistry (Positive): Distonic Radical Cations*). SX135 01045

The second example illustrates reorientation of the ion. Ionization of carbonate esters gives rise to expulsion of CO_2. Scheme 6 summarizes the experimental result for phenyl *s*-butyl carbonate. Stereoisotopic labeling demonstrates that loss of CO_2 gives ionized phenyl *s*-butyl ether with inversion of configuration at the asymmetric center (<Bib18>*18*). This has to take place via heterolysis of an oxygen–carbon bond followed by reorientation of the ionic fragment. Subsequent nucleophilic displacement via backside attack (represented by the solid curved arrow) generates the observed daughter ion. SX140

The third example illustrates reorientation of both partners within an ion–neutral complex. Alkyl 4-pyridyl ether radical cations undergo double hydro- SX145

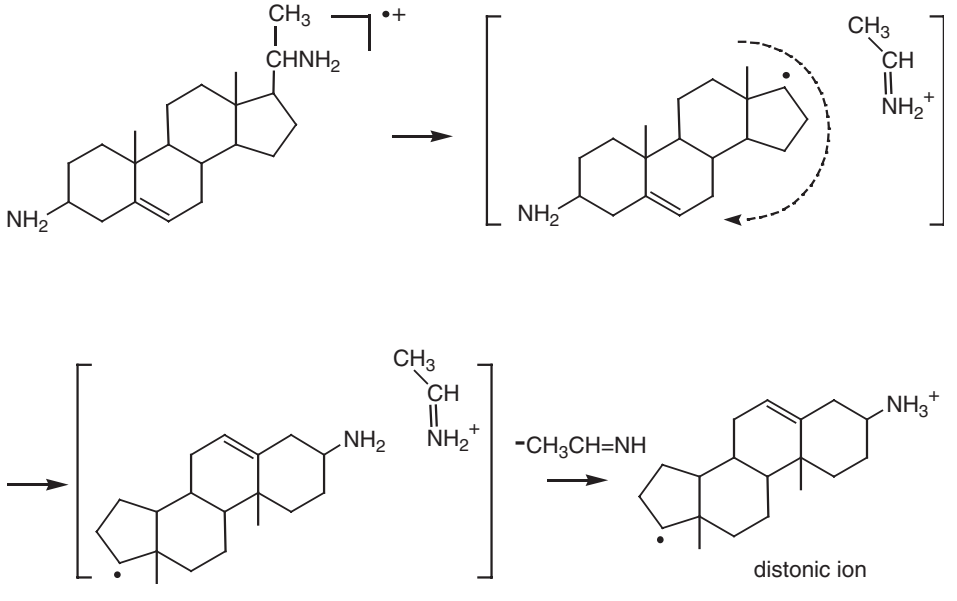

Scheme 5

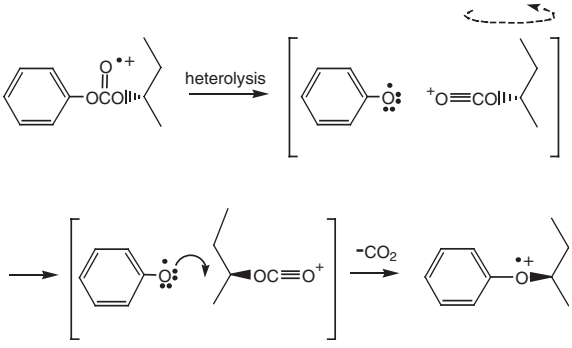

Scheme 6

gen transfers via ion–neutral complexes, expelling allylic radicals to produce protonated hydroxypyridine, *m*/*z* 96 (<Bib19>*19*). Scheme 7 depicts the double hydrogen transfer that takes place when cyclooctyl 4-pyridyl ether is ionized at low energy. An sp^3 carbon–oxygen bond heterolyzes, forming a cyclooctyl cation. In this cation, a hydrogen at position 5 bridges over to position 1, introducing a new element of symmetry. Position 2 becomes equivalent to position 4, and position 6 becomes equivalent to position 8. Deuterium labeling shows that the ionic fragment turns so as to render the newly equivalent positions equally accessible to the neutral partner (a pyridyloxy radical). The radical turns so that its nitrogen receives a proton to form a second complex containing cyclooctene and ionized 4-pyridone. After this proton transfer, the aromatic fragment executes another turn and its oxygen abstracts a hydrogen, yielding *m*/*z* 96 as the most abundant fragment ion (<Bib20>*20*).

SX150 The fourth example illustrates a case where a complex returns to a covalent intermediate following reorientation. The ionized ketone in Scheme 8 tautomerizes to a distonic ion and undergoes subsequent cleavage to expel 1,3-butadiene in a conventional McLafferty rearrangement. However, a thermodynamically preferred pathway involves further isomerization of the distonic ion (see *Organic* 01045 *Ion Chemistry (Positive): Distonic Radical Cations*) and expulsion of an ethyl radical. This latter isomerization passes through several distonic structures and proceeds slowly compared to the McLafferty rearrangement. Ions that do not have enough energy to complete the McLafferty rearrangement form ion–neutral complexes containing the McLafferty fragments. Reorientation of the butadiene partner and recombination interchanges chain positions 3 and 4 with positions 6 and 5, respectively. Isotopic labeling of carbon atoms reveals that this interchange takes place prior to metastable ion decompositions that expel ethyl radical (<Bib21>*21*). Parenthetically, it should be added that ion–neutral complexes created by McLafferty rearrangements of other carbonyl compounds can lead to "McLafferty + 1" peaks when the enol radical cation abstracts a hydrogen atom from an sp^3 carbon of its neutral partner (<Bib22>*22*).

2.3 Rearrangements within Ion–Neutral Complexes SX155

The most salient feature of ion–neutral complexes is that they permit rearrangements and reactions that could not take place from their covalent precursors. The first recognized examples of ion–neutral complexes were uncovered during studies of metastable oxonium ions, which expel water (<Bib22>*22*). As Scheme 9 depicts, this decomposition requires a deep-seated rearrangement via two successive ion–neutral complexes. First a bond heterolysis forms a complex containing a cation and formaldehyde (often with

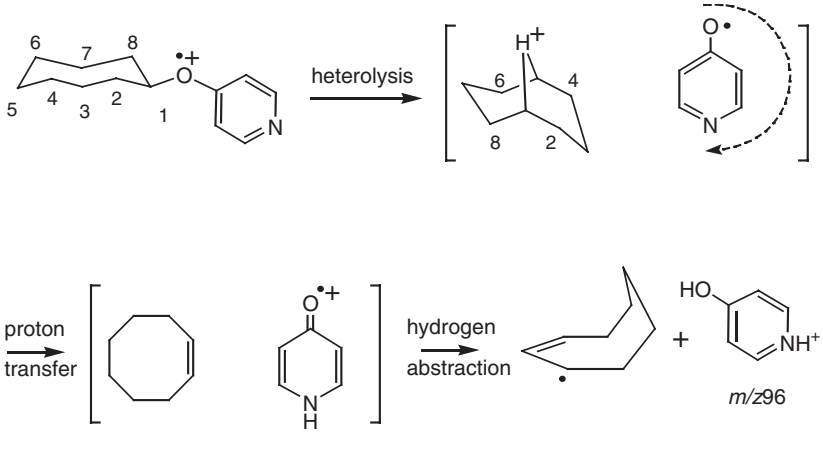

Scheme 7

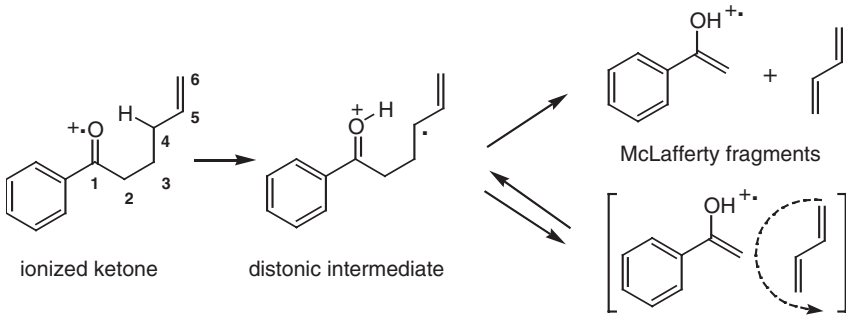

Scheme 8

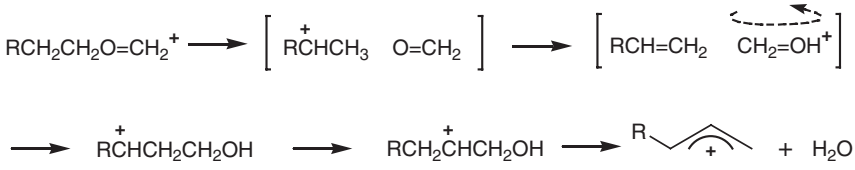

Scheme 9

alkyl rearrangement). Then proton transfer produces a complex containing alkene and hydroxymethyl cation. *Ab initio* calculations (<Bib23>*23*) on the simplest case (R = H) predict an energy barrier of the order of 100 kJ mol^{-1} for reorientation of the hydroxymethyl cation within the complex (represented by the dashed arrow). Re-addition of the reoriented hydroxymethyl cation to the alkene gives an O-protonated carbonyl compound, from which elimination of water takes place to yield an allylic cation.

O-protonated carbonyl compounds can themselves SX160
decompose via ion–neutral complexes. Metastable ion decomposition of the conjugate acid from neopentyl methyl ketone gives *t*-butyl cation, but, as the deuterium labeling experiment drawn in Scheme 10 summarizes, only a small fraction of those ions come from simple cleavage. The initial bond fission forms the enol of acetone, which remains in a complex and undergoes hydron (H^+/D^+) exchange with its partner so as to yield the keto

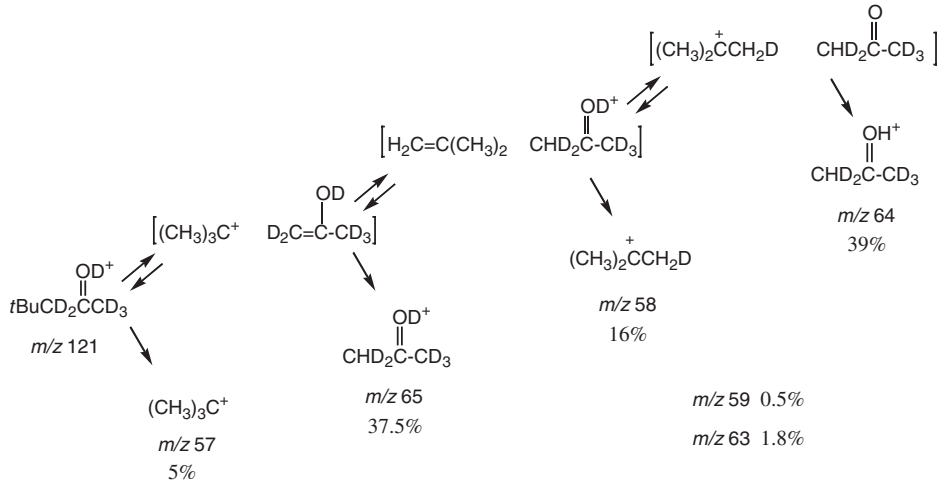

Scheme 10

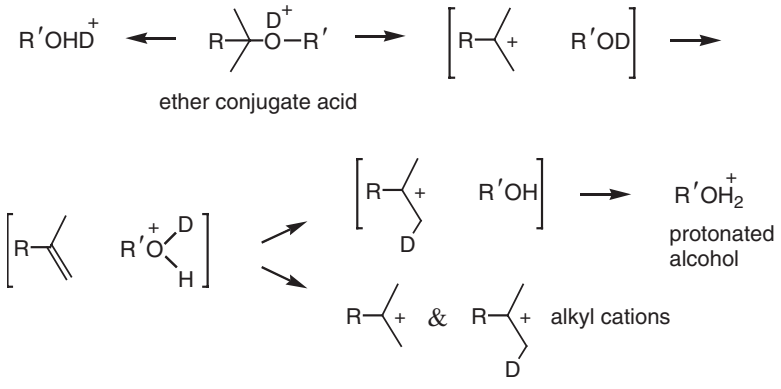

Scheme 11

tautomer as the expelled neutral (<Bib24>*24*). The sequence of intermediates in Scheme 10 produces acetone conjugate acid ions, whose distribution of label also attests to the sequence of interconverting ion–neutral complexes.

SX165 Analogous bond heterolysis takes place within ether conjugate acid ions. Here, rearrangement does not necessarily occur, but the intermediacy of ion–neutral complexes is demonstrated by hydron exchange, as the sequence of reactions to the right in Scheme 11 depicts. Simple aliphatic ethers, such as methyl *t*-butyl ether (MTBE, R = R′ = methyl) tend to give alkyl cations in which the D originally deposited on oxygen has been incorporated into the hydrocarbon (<Bib25>*25*).

SX170 When R′ is aromatic, protonated phenol ions (in place of protonated alcohols) dominate the product distribution. Some debate has arisen as to whether the precursor ether conjugate acid ions are ring protonated (like the *ipso*-protonated ion in Scheme 3) or O-protonated (like the conjugate acid ion in Scheme 11). Analysis of product distributions from a variety of deuterated conjugate acids from 2-phenoxypropane (R = H, R′ = phenyl in Scheme 11) has demonstrated that O-protonated ions are the precursors of the ion–neutral complexes from aryl alkyl ethers, just as they are from dialkyl ethers (<Bib26>*26*).

SX175 Hydrogen exchange between the partners in a complex can also occur in odd-electron ions. Atom abstraction from propane by ionized vinyl alcohol is nearly thermoneutral; hence, the formation of an ion–neutral complex containing those two partners leads to the reversible interconversion summarized in Scheme 12, in which the center atom of the expelled propane (which originates from position 3 of the precursor) scrambles hydrogen with the methyl originating from position 1 (<Bib27>*27*).

SX180 Heterolysis of an odd-electron precursor can give rise to hydrogen exchange, as well. For instance, ionized neopentyl methyl ether heterolyzes to create an ion–neutral complex containing *t*-butyl cation and a methoxymethyl radical. As Scheme 13 depicts, all the hydrogens scramble as a consequence of the interchange between this complex and one containing dimethyl ether and ionized isobutene (<Bib27>*27*).

In the foregoing discussion, the distinction between SX185 homolysis and heterolysis in odd-electron ions might seem to be a mere formalism, because charge and spin can delocalize between two partners in close proximity. Homolysis and heterolysis from a given precursor, however, produce ion–neutral complexes with different electronic structures. This distinction has been tested by means of characteristic cyclization chemistry. The 5-hexenyl system yields products with ring sizes that depend on whether it is a cation or a

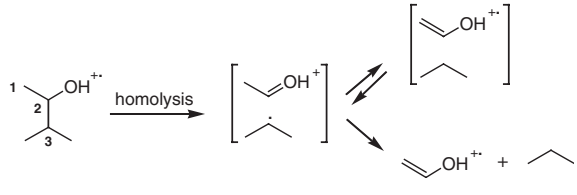

Scheme 12

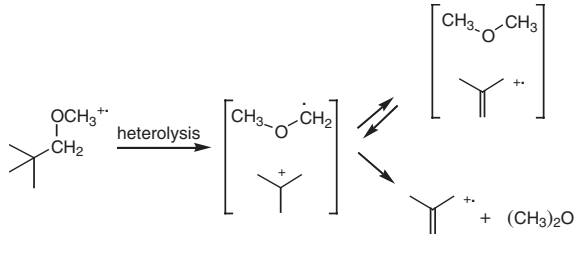

Scheme 13

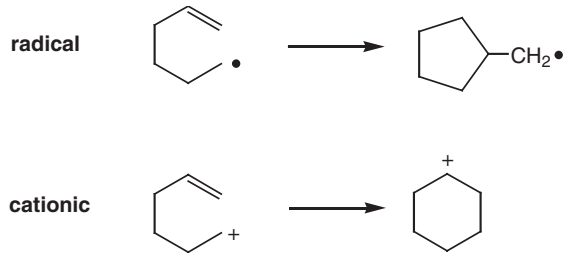

Scheme 14

free radical, as Scheme 14 summarizes. 5-Hexenyl radicals close to form cyclopentylmethyl radicals, whereas 5-hexenyl cations close to form cyclohexyl cations. Ionized phenyl 5-hexenyl ether, $CH_2=CHCH_2CH_2CH_2CH_2OPh^{\bullet+}$, expels neutral C_6H_{10} to give $PhOH^{\bullet+}$. The deuterated precursor $CD_2=CHCH_2CH_2CH_2CH_2OPh$ gives $PhOD^{\bullet+}$ as well as $PhOH^{\bullet+}$.

SX190 The expelled uncharged fragments have been collected in a specially designed electron bombardment flow (EBFlow) reactor, which is illustrated schematically in Fig. 3. The EBFlow reproduces the conditions in an electron ionization mass spectrometer source, but with a distance between the electron source and the target that is nearly 1 m long. Reactant gases (at pressures [10^{-3} torr]) flow continuously along the path of the electron beam, which is kept from diverging by a coaxial magnetic field. Neutral products are collected in a cold trap and subsequently analyzed by gas chromatography or NMR.

SX195 EBFlow experiments on primary alkyl phenyl ethers show evidence of rearrangements that are characteristic of intermediate ion–neutral complexes containing a phenoxy and a hydrocarbon fragment. If the complex from $CH_2=CHCH_2CH_2CH_2CH_2OPh\cdot^+$ had the electronic structure corresponding to initial bond homolysis, $[PhO^+ \cdot C_6H_{11}\cdot]$, five-membered ring products, such as methylenecyclopentane, would have been expected among the expelled neutrals. By contrast, complexes resulting from initial bond heterolysis should have the structure $[PhO\cdot C_6H_{11}^+]$ and ought to produce cyclohexene among the collected neutral products. These two alternatives represent different electronic states of the ion–neutral complex. The experimental results show cyclohexene and no five-membered ring neutral products (<Bib28>*28*). In general, ion–neutral complexes from odd-electron precursors arise either via homolysis (as in Schemes 1 and 12) or via heterolysis (as in Schemes 6 and 7) and rarely display evidence for two electronic states in competition with one another.

SX200 By contrast, competing rearrangement pathways have been observed in the formation of ion–neutral complexes, giving different structural isomers. When

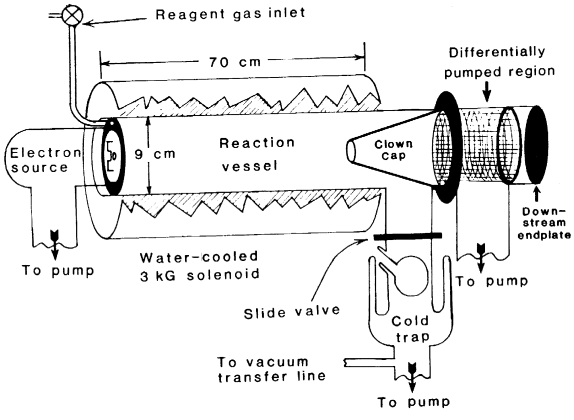

Figure 3
Schematic diagram of an electron bombardment flow (EBFlow) reactor. An external solenoid electromagnet keeps the electrons on the axis of the cylindrical reaction vessel, and the electrical charge of the beam (along with the magnetic field) prevents collisions from driving positive ions to the walls. At the far end of the vessel, electrons and ions exit to a differentially pumped chamber via a conical Faraday plate ("clown cap"), while neutrals find their way into a liquid nitrogen-cooled trap, where they are collected. The efficiency of neutral product collection has been estimated to be of the order of 85% (reproduced by permission from *J. Org. Chem.* **2000**, *65*, 8032–8040).

ionized, many 1-phenoxyalkyl compounds heterolyze to form ion–neutral complexes containing rearranged alkyl cations and a phenoxy radical. Schemes 15–17 illustrate cases where the competition between the formation of two different ion–neutral complexes has been investigated in detail, using both mass spectrometry and EBFlow techniques.

Scheme 15 portrays a cationic isomerization pathway that is well known from solution-phase chemistry, called a Wagner–Meerwein rearrangement. When X = methyl, the two pathways in Scheme 15 are identical and indistinguishable, although two different neutral products are recovered in an EBFlow experiment (<Bib29>*29*). The two isomeric 2-methylbutenes are produced in roughly the same ratio as is formed by deprotonation of free, gaseous *t*-pentyl cation, as one might expect from a Brønsted acid–base reaction between the partners in the complex, forming ionized phenol as the fragment ion detected in the mass spectrometer. When X = F in Scheme 15, the competing Wagner–Meerwein pathways (methyl shift versus fluorine shift) yield different neutral alkenes, and all of the neutral products shown in Scheme 15 are found in an EBFlow experiment (<Bib30>*30*). SX205

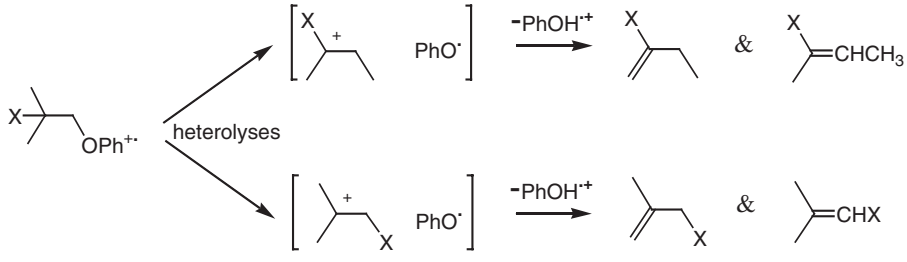

Scheme 15

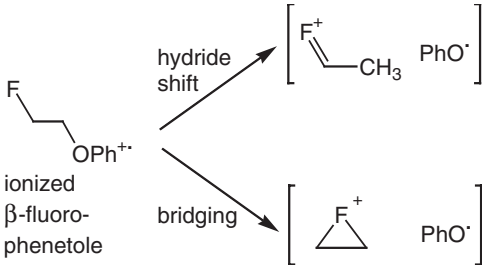

Scheme 16

SX210 This leads to the question as to whether fluorine migration takes place via a bridged fluoronium ion. Evidence for that kind of bridging emerges from EBFlow studies of ionized β-fluorophenetole, as Scheme 16 summarizes (<Bib31>*31*). Two competing rearrangement pathways operate, both leading to the expulsion of neutral vinyl fluoride to form ionized phenol. However, analysis of the deuterium content of the neutral products from specifically labeled precursors demonstrates that 1,2-hydride shift and fluorine bridging function as distinct, nonsequential pathways in the formation of ion–neutral complexes.

SX215 In the next higher homologue, shown in Scheme 17, two different initial hydride shifts compete with one another. Both pathways—1,2-hydride shift and 1,3-hydride shift—lead to the same interconverting pair of isomeric ion–neutral complexes. The relative contributions of the two competing mechanisms can be measured by looking at a specifically deuterated precursor. The placement of isotopic label in the neutral 1-fluoropropenes recovered in an EBFlow experiment shows that 1,2-shift operates about 15 times more often than 1,3-shift (<Bib32>*32*). The phenomenon of multiple pathways to the same complex is not uncommon (<Bib33>*33*), and some effort has gone into determining the relative contributions of competing mechanisms by means of isotopic labeling.

3. Can Ion–Neutral Complexes be Predicted? SX220

The sampling of complex-mediated reactions presented here gives an idea of the scope of this class of mechanisms. Although there are many other examples (some with more than one neutral partner—so called terbody complexes (<Bib34>*34*, <Bib35>*35*)), it is fair to say that the majority of gas-phase ion decompositions are not complex mediated and take place via simple cleavages, distonic ion rearrangements, or other more conventional types of pathways (see *Organic Ion Chemistry (Positive): Distonic Radical Cations*). What, then, are the properties that determine whether an ion complex operates in a unimolecular decomposition? As originally conceived, three criteria were viewed as having particular relevance (<Bib36>*36*): 01045

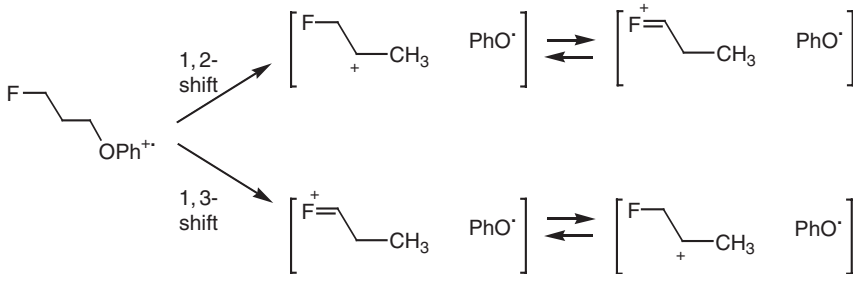

Scheme 17

(i) the precursor must be singly charged (because fragments with charges of the same sign repel one another);

(ii) the weakest bond of the precursor dissociates to give the complex (and the corresponding simple cleavage fragments are also often observed); and

(iii) the partners within the complex have to be able to undergo an ion–molecule reaction with each other.

SX225 It is now clear, however, that the second of these criteria is not essential. In the decomposition of ionized acetamide, for instance, other homolyses compete with the cleavage symbolized in Scheme 1: e.g., formation of $[CH_3C{\equiv}O^+NH_2\cdot\ ]$ complexes, which lead to expulsion of ammonia or of carbon monoxide (<Bib37>*37*). Nevertheless, as discussed in Sect. 1.3, a density-of-states model makes a reasonable quantitative prediction of the relative probability of forming $[O=C=NH_2^+CH_3\cdot\ ]$ complexes.

SX230 Despite the success of this approach (<Bib7>*7*, <Bib8>*8*), it seems that no purely statistical model is likely to give a complete picture. The ratio of alkane to alkyl radical expulsion in isomeric radical cations shows a dependence on the site of cleavage (<Bib11>*11*, <Bib38>*38*), which contradicts what one would expect if internal energy quickly randomizes over all internal degrees of freedom. Such a dependence implies an impulsive effect: namely, that the ''kick'' given one of the fragments during bond fission imparts to it an angular momentum that persists for the duration of the ion–neutral complex.

SX235 Other questions also remain to be answered. For instance, protonated ethers of all types decompose via complexes, as typified in Scheme 11. In the same vein, ionized alkyl 4-pyridyl ethers (as in Scheme 7) and primary alkyl phenyl ethers (as in Schemes 15–17) expel hydrocarbon fragments exclusively by heterolysis to form complexes. Yet this represents only a minor pathway for alkene expulsion from ionized secondary alkyl phenyl ethers (<Bib39>*39*, <Bib40>*40*). Nor is it apparent, as of this writing, how large a translational kinetic energy release ought to be expected for the final products of a complex-mediated reaction (although much has been published on the subject (<Bib36>*36*, <Bib41> <Bib42> <Bib43>*41–43*)). As electronic databases of mass spectrometric fragmentations grow to include ever-larger ions (and as computer-assisted analyses of these databases proliferate), a more detailed understanding of ion–neutral complexes will surely develop. These sorts of questions will have to be addressed if mass spectrometry is to fulfill its promise as a stand-alone method of structural determination.

Acknowledgments

The support of NSF grant CHE9983610 is gratefully acknowledged.

Bibliography

<Bib1>(*1*) Abboud, J. L. M.; Alkorta, I.; Davalos, J. Z.; Gal, J. F.; Herreros, M.; Maria, P.-C.; Mó, O.; Molina, M. T.; Notario, R.; Yáñez, M. The $P_4\,Li^+$ Ion in the Gas Phase: A Planetary System. *J. Am. Chem. Soc.* **2000**, *122*, 4451–4454.

<Bib2>(*2*) Midland, M. M.; Morton, T. H. Is Protonated Ammonium Fluoride an Ion–Neutral Complex in the Gas Phase? *J. Am. Chem. Soc.* **1993**, *115*, 9596–9601.

<Bib3>(*3*) Illies, A. J.; Morton, T. H. Strong Hydrogen Bonding in the Gas Phase: Fluoromethane…Hydronium *versus* Fluoromethane…Ammonium. *Int. J. Mass Spectrom. Ion Proc.* **1997**, *167/168*, 431–445.

<Bib4>(*4*) Norrman, K.; McMahon, T. B. Generation of Covalent and Electrostatic Complexes in Association Reactions of *tert*-Butyl Cation with Small Organics. *J. Am. Chem. Soc.* **1996**, *108*, 2449–2457.

<Bib5>(*5*) Longevialle, P. Ion–Neutral Complexes in the Unimolecular Reactivity of Organic Cations in the Gas Phase. *Mass Spectrom. Rev.* **1992**, *11*, 157–192.

<Bib6>(*6*) Baer, T.; Hase, W. L. *Unimolecular Reaction Dynamics: Theory and Experiments*; Oxford University Press: New York, 1996; pp. 227–228.

<Bib7>(*7*) Morton, T. H. Competition in the Formation of Ion–Neutral Complexes. Expulsion of Methane from the Molecular Ion of Acetamide. *Org. Mass Spectrom.* **1991**, *26*, 18–23.

<Bib8>(*8*) Chronister, E. L.; Morton, T. H. Internal Energy Effects on Ion–Neutral Complexes from Unimolecular Dissociation of *n*-Propyl Phenyl Ether Radical Cations. *J. Am. Chem. Soc.* **1990**, *112*, 133–139.

<Bib9>(*9*) Schröder, D.; Loos, J.; Thissen, R.; Dutuit, O.; Mourgues, P.; Audier, H. E.; Lifshitz, C.; Schwarz, H. Barrier Height Titration by Tunable Photoionization Combined with Chemical Monitoring: Unimolecular Keto/Enol Tautomerization of the Acetamide Cation Radical. *Angew. Chem. Int. Ed.* **2002**, *41*, 2748–2751.

<Bib10>(*10*) McAdoo, D. J.; Bowen, R. D. Alkane Eliminations from Ions in the Gas Phase. *Eur. Mass Spectrom.* **1999**, *5*, 389–409.

<Bib11>(*11*) McAdoo, D. J.; Hudson, C. E.; Traeger, J. C.; Giam, C. S. Dependency of H-transfer on the Initial Configuration of the Partners in Ion–Neutral Complexes: Motion of the Partners as a Function of the Initial Geometry of Complexes. *Int. J. Mass Spectrom. Ion Proc.* **1997**, *167/168*, 425–429.

<Bib12>(*12*) Tumas, W. H.; Foster, R. F.; Brauman, J. I. Mechanistic Studies of Gas-phase Negative Ion Unimolecular Decompositions. Alkoxide Ions. *J. Am. Chem. Soc.* **1988**, *110*, 2714–2722.

<Bib13>(*13*) Kuck, D. Half a Century of Scrambling in Organic Ions: Complete, Incomplete, Progressive, and Composite Atom Interchange. *Int. J. Mass Spectrom.* **2002**, in press.

<Bib14>(*14*) Matthias, C.; Anlauf, S.; Weniger, K.; Kuck, D. Gaseous [t-$C_4H_9^+$ α,ω-diphenylalkane] Complexes: Methyl Substitutent Effects on the Intracomplex Proton

Transfer and Regio-selective Hydride Abstraction. *Int. J. Mass Spectrom.* **2000**, *199*, 155–187.

<Bib15>(*15*) Mayer, P. S.; Leblanc, D.; Morton, T. H. Gas Phase Halonium Metathesis and its Competitors. Skeletal Rearrangements of Cationic Adducts of Saturated Ketones. *J. Am. Chem. Soc.* **2002**, in press.

<Bib16>(*16*) McAdoo, D. J.; Morton, T. H. Gas Phase Analogues of Cage Effects. *Acc. Chem. Res.* **1993**, *26*, 295–302.

<Bib17>(*17*) Audier, H. E.; Morton, T. H. Backside Displacement in the Unimolecular Gas Phase Decarboxylation of Alkyl Phenyl Carbonate Radical Cations. *J. Am. Chem. Soc.* **1991**, *113*, 9001–9003.

<Bib18>(*18*) Molenaar-Langeveld, T. S.; Gremmen, C.; Ingemann, S.; Nibbering, N. M. M. Isomeric Dependences of the Formation of Ion/Neutral Complexes in Dissociation Reactions of Ionized Propoxypyridines. *Int. J. Mass Spectrom.* **2000**, *199*, 1–16.

<Bib19>(*19*) Biermann, H. W.; Freeman, W. P.; Morton, T. H. Ion–Molecule Complexes in Decomposition of Gaseous Cations: 130 nm photolysis of 4-Pyridyl Ethers. *J. Am. Chem. Soc.* **1982**, *104*, 2307–2308.

<Bib20>(*20*) Morton, T. H. The Reorientation Criterion and Positive Ion–Neutral Complexes. *Org. Mass Spectrom.* **1992**, *27*, 353–368.

<Bib21>(*21*) Dohmeier-Fischer, S.; Kramer, N.; Grützmacher, H. F. Rearrangement by Intermediate Ion/Neutral Complexes During the McLafferty Fragmentation of Unsaturated Ketones. *Eur. Mass Spectrom.* **1995**, *1*, 3–10.

<Bib22>(*22*) Bowen, R. D. Ion–Neutral Complexes. *Acc. Chem. Res.* **1991**, *12*, 364–371.

<Bib23>(*23*) Chalk, A. J.; Radom, L. The Importance of Ion–Neutral Complexes in Gas-phase Ionic Reactions: Fragmentation of $[CH_3CH_2OCH_2]^+$ as a Prototypical Case. *J. Am. Chem. Soc.* **1998**, *120*, 8430–8437.

<Bib24>(*24*) Kong, J.; Mayer, P. S.; Morton, T. H. Carbocation Rearrangements of Trimethylsilyl Adducts of Saturated Acyclic C_5–C_7 Ketones in the Gas Phase. *Int. J. Mass Spectrom.* **2002**, *217*, 257–271.

<Bib25>(*25*) Audier, H. E.; Berthomieu, D.; Morton, T. H. Gas Phase Decomposition of Conjugate Acid Ions of Simple *tert*-Butyl Alkyl Ethers. *J. Org. Chem.* **1995**, *60*, 7198–7208.

<Bib26>(*26*) Audier, H. E.; Morton, T. H. Ring *versus* Oxygen Protonation in Metastable Ion Decompositions of Protonated Isopropyl Phenyl Ether. *Int. J. Mass Spectrom.* **1999**, *185/187*, 393–399.

<Bib27>(*27*) Hammerum, S.; Audier, H. E. Experimental Verification of the Intermediacy and Interconversion of Ion–Neutral Complexes as Radical Cations Dissociate. *J. Chem. Soc. Chem. Commun.* **1988**, 860–861.

<Bib28>(*28*) Hall, D. G.; Morton, T. H. Ion–Molecule Complexes in Unimolecular Fragmentations of Gaseous Cations. Cyclization of Unsaturated Carbocations in the Gas Phase. *J. Am. Chem. Soc.* **1980**, *102*, 5686–5688.

<Bib29>(*29*) Morton, T. H. Ion–Molecule Complexes in Unimolecular Fragmentations of Gaseous Cations. Alkyl Phenyl Ether Molecular Ions. *J. Am. Chem. Soc.* **1980**, *102*, 1596–1602.

<Bib30>(*30*) Shaler, T. A.; Morton, T. H. Fluorine Shifts in Gaseous Cations. Analogues of Wagner–Meerwein Rearrangements. *J. Am. Chem. Soc.* **1994**, *116*, 9222–9226.

<Bib31>(*31*) Nguyen, V.; Cheng, X.; Morton, T. H. 3-Member Cyclic Fluoronium Ions in Gaseous Ion–Neutral Complexes. *J. Am. Chem. Soc.* **1992**, *114*, 7127–7132.

<Bib32>(*32*) Shaler, T. A.; Borchardt, D.; Morton, T. H. Competing 1,3- and 1,2-Hydrogen Shifts in Gaseous Fluoropropyl Cations. *J. Am. Chem. Soc.* **1999**, *121*, 7907–7913.

<Bib33>(*33*) Traeger, J. C.; Morton, T. H. Mechanisms for the Expulsion of Propene from Ionized Propyl Phenyl Ethers in the Gas Phase. *J. Am. Chem. Soc.* **1996**, *118*, 9661–9668.

<Bib34>(*34*) Audier, H. E.; Berthomieu, D.; Leblanc, D.; McMahon, T. B.; Morton, T. H. Ion–Molecule Reactions of *tert*-Butyl Cation with Tertiary Alcohols. *Int. J. Mass Spectrom. Ion Proc.* **1992**, *17*, 327–344.

<Bib35>(*35*) Tu, Y. P.; Holmes, J. L. Ion–Neutral–Neutral Complexes in Unimolecular Reactions: Formation of Proton–Bound Alkanol Pairs from Alkoxylated Oxonium Ions. *J. Chem. Soc. Perkin Trans. II* **2001**, 1378–1382.

<Bib36>(*36*) Morton, T. H. Gas Phase Analogues of Solvolysis Reactions. *Tetrahedron* **1982**, *38*, 3195–3243.

<Bib37>(*37*) Drewello, T.; Heinrich, N.; Maas, W. P. M.; Nibbering, N. M. M.; Weiske, T.; Schwarz, H. Generation of the Distonic Ion $\cdot CH_2NH_3^+$: Nucleophilic Substitution of the Ketene Cation Radical by Ammonia and Unimolecular Decarbonylation of Ionized Acetamide. *J. Am. Chem. Soc.* **1987**, *109*, 4810–4818.

<Bib38>(*38*) Longevialle, P.; Lefevre, O.; Mollova, N.; Bouchoux, G. Further Arguments Concerning a "Rotational Effect" in the Unimolecular Fragmentations of Organic Ions in the Gas Phase. *Rapid Commun. Mass Spectrum.* **1998**, *12*, 57–60.

<Bib39>(*39*) Traeger, J. C.; Luna, A.; Tortajada, J. C.; Morton, T. H. Regio- and Stereochemistry of Alkene Expulsions from Ionized *sec*-Alkyl Phenyl Ethers. *J. Phys. Chem. A* **1999**, *103*, 2348–2358.

<Bib40>(*40*) Morizur, J. P.; Taphanel, M. H.; Mayer, P. S.; Morton, T. H. Stereochemical Analysis of Deuterated Alkyl Chains by MS/MS. *J. Org. Chem.* **2000**, *65*, 381–387.

<Bib41>(*41*) Schwarz, H.; Stahl, D. Unimolecular Water Loss from Protonated Alcohols in the Gas Phase: The Effect of Ion/Dipole Interactions on the Isomerizations of Incipient Carbocations. *Int. J. Mass Spectrom. Ion Phys.* **1980**, *136*, 285–289.

<Bib42>(*42*) Bowen, R. D. Unimolecular Reactions of Isolated Organic Ions: Olefin Elimination from Immonium Ions $R^1R^2N^+=CH_2$. *J. Chem. Soc. Perkin Trans. II* **1982**, 409–413.

<Bib43>(*43*) Hammerum, S.; Hansen, M. M.; Audier, H. E. On the Release of Translational Energy when Stable Intermediate Ion–Neutral Complexes Dissociate. *Int. J. Mass Spectrom. Ion Proc.* **1997**, *160*, 183–192.

T. H. Morton
University of California
Riverside, California
USA

Title: Encyclopedia of Mass Spectrometry (EMAS)
Article/Number: Collisional Activation and Dissociation: Via Ion-neutral Complexes/01064

ELSEVIER

Dear Author,
During the preparation of your manuscript for typesetting some questions have arisen. These are listed below. Please check your typeset proof carefully and mark any corrections in the margin of the proof or compile them as a separate list. This form should then be returned with your marked proof/list of corrections to Elsevier Science.

Information in margins: "SX000" codes relates to the subject index and "6-digit numbers" refer to cross-references to other articles in EMAS.

This form should then be returned with your marked proof/list of corrections to Jerome Michalczyk (j.michalczyk@elsevier.com; fax no. +44 (0) 1865 843974) at Elsevier Science Ltd., Major Reference Works, The Boulevard, Langford Lane, Kidlington, Oxford OX5 1GB.

Queries and/or remarks

No Queries